Effect of Ions on the Polymorphism, Effective Charge, and Stability of Human Telomeric DNA. Photon Correlation Spectroscopy and Circular Dichroism Studies

Agnieszka Włodarczyk,*,† Przemysław Grzybowski,‡ Adam Patkowski,† and Andrzej Dobek†

Faculty of Physics, Molecular Biopysics Division, and Faculty of Physics, Solid State Theory Division, A. Mickiewicz University, Umultowska 85, 61−614 Poznań, Poland

Received: October 15, 2004; In Final Form: December 13, 2004

The effect of different ions on the formation and behavior of quadruplex structures of the human telomere sequence d(TTAGGG)$_4$ has been studied by photon correlation spectroscopy (PCS) and circular dichroism (CD). The saturation and melting curves obtained in the presence of K^+, Na^+, Rb^+, Li^+, Cs^+, and Sr^{2+} ions were recorded by CD spectroscopy and indicated the formation of monomeric quadruplexes. Analysis of the saturation curves obtained at 2 °C has shown that the presence of a single Sr^{2+} ion per oligomer is sufficient for the formation of a monomeric quadruplex of the DNA sequence studied. In the presence of $SrCl_2$ at a concentration of 50 mM, the formation of tetrameric quadruplexes has been detected. The effect of Sr^{2+} ions on the formation of quadruplex structures by the human telomere sequence d(TTAGGG)$_4$ is stronger and different from that of the other ions tested. The paper also presents results of a study of electrostatic interactions in solution. The translation diffusion coefficients D_T of the structures present in solution have been determined by photon correlation spectroscopy and the effective charges on the structures have been calculated by combining the experimental data with the results based on the coupled mode theory. Analysis of the melting points monitored by the CD method has permitted a determination of Δn, the number of ions released in the process of thermal denaturation. All the results are in good agreement with the predictions based on the theory of polyelectrolytes. The effect of ions on the formation and behavior of quadruplex structures of the human telomere sequence d(TTAGGG)$_4$ has been studied by photon correlation spectroscopy and circular dichroism.

I. Introduction

Human telomeric DNA, located on the end of chromosomes, consists of repeats of the (TTAGGG/CCCTAA) sequence and ends in the single strand by TTAGGG, which protrudes beyond the double stranded DNA helix. These single G-rich strands are known to form in vitro, in the presence of specific alkali cations, unique four stranded helical conformations that are called quadruplexes. The structure of the human telomere sequence d[$AG_3(T_2AG_3)_3$] in Na^+-containing solution has been determined using a combined NMR, distance geometry, and molecular dynamics approach.[1] This sequence with four copies of AG_3 repeats folds intramolecularly into monomeric G-quadruplex stabilized by three stacked G-tetrads with guanine *syn-anti* along the individual strand and *syn-anti-anti-syn* around the individual G-tetrad. G-tetrads are connected by two lateral loops and a central diagonal loop (Figure 1a). Henceforth in the paper this structure is referred to as the antiparallel monomeric quadruplex. Interestingly, crystal structure determinations of the same sequence in the presence of K^+ ions have revealed a new quadruplex topology[2] where three tetrads stacked one upon another are all oriented in the same direction, and the three connecting loops are of the double-chain reversal type (Figure 1b). This structure will be referred to as the parallel monomeric quadruplex. The same parallel-stranded alignment of the two-repeat sequence of human telomeric DNA has been observed.[2] The reason for the difference in Na^+- and K^+-monomeric quadruplex topology can be due to different coordination geometries around these two ions in the telomeric structure. As pointed out previously, the K^+-stabilized monomeric quadruplex can have implications for higher order structures via stacking of disklike quadruplexes.[2]

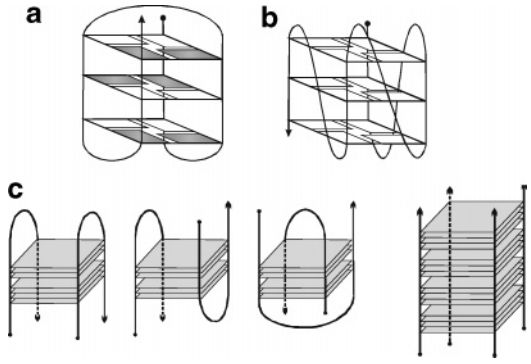

Figure 1. Schematic drawing of the quadruplex structures that can be adopted by the telomeric G-strand sequence d[$AG_3(T_2AG_3)]_4$: (a) The Na^+ stabilized solution structure: anti-parallel monomer.[1] Solid and dashed lines represent the sugar phosphate backbone. A solid circle indicates the 5′ end of the strand and an arrow indicates the 3′ end of the strand. Bases indicated by shaded rectangles are in the syn glycoside bond conformation of the glycoside torsion angle while those with unshaded rectangles are in the anti conformation. (b) The K^+ stabilized crystal structure: parallel monomer described by Parkinson et al.[2] (c) Dimers considered in the study. (d) Tetramer. Shaded squares in parts c and d represent guanine quartets.

* Address correspondence to this author. Current address: Davy-Faraday Research Laboratory, Royal Institution of Great Britain, 21 Albemarle Street, London W1S 4BS, UK. Phone: +00 44 20 7670 2919, +00 44 20 7679 4557. Fax: +44 20 7629 2920. E-mail: agnieszka@ri.ac.uk.

† Faculty of Physics, Molecular Biopysics Division.

‡ Faculty of Physics, Solid State Theory Division.

10.1021/jp045274d CCC: $30.25
Published on Web 02/01/2005

Using NMR spectroscopy it was shown that two-repeat telomeric sequence $d(TAGGGT)_2$ can form both parallel and antiparallel G-quadruplex structures in K^+-containing solution. Both structures are dimeric G-quadruplexes involving three stacked G-tetrads and they can coexist and interconvert in solution. They also have different thermodynamic properties and different kinetics of folding and unfolding.[3]

The structural properties of human telomeric repeat oligonucleotide models consisting of two runs of GGG: $d(G_3T_2AG_3)$ and four runs of GGG: $d(T_2AG_3)_4$, $d(G_3T_2A)_3G_3$, in solution in the presence of Na^+ and K^+, were also investigated using CD, gel electrophoresis, and chemical probing techniques.[4] The sequence with four runs of GGG assumes an intramolecular folded-back monomeric quadruplex, whereas the sequences with two runs of GGG adopt an antiparallel G-quadruplex by dimerization of hairpins. Sodium-induced quadruplexes differ from their potassium-induced counterparts in the stability, loop conformation, and interactions.[4] Further, the higher order DNA structure can be formed by the association of two hairpin dimers via stacking of G-tetrad planes.[4,5]

The structural nature of complexes formed by the human telomeric sequence $d(5'\text{-}TTAGGG\text{-}3')_4$ is now determined; however, much less is known about the interactions between and within these structures in solutions. The first problem that must be addressed concerns the effects of electrostatic interactions, as the DNA molecules in neutral pH are highly charged polyions. This problem has been studied here by the photon correlation spectroscopy method that permits determination of the translational diffusion coefficients D_T of the collective diffusion modes associated with the DNA molecules in solution. Together with the results of the calculations based on the coupled mode theory, this method permits also determination of the effective charges of the structures studied. Supplementing the experimental information with an analysis of the hydrodynamic parameters of the molecules, we are able to conclude the shape and size of the structures in solution and also to estimate relative weight concentrations of the structures observed. Also the effect of K^+, Na^+, Rb^+, Li^+, Cs^+, Ca^{2+}, Mg^{2+}, and Sr^{2+} ions on formation of the quadruplex structures by the human telomeric sequence $d(TTAGGG)_4$ was analyzed by CD spectroscopy and compared.

II. Theoretical Basis

The Coupled Mode Theory. The coupled mode theory[6,7] describes the collective diffusion of electrically charged molecules taking into account the electrostatic interactions between small cations and anions, large polyions, and between polyions and small ions, disregarding all other types of interactions. Here we present a brief summary of the method. Let a polyion of charge Z_pe, where e is the elementary electric charge, have a diffusion coefficient D_p. Let the counterions (cations and anions) have charges and diffusion coefficients of Z_ce, D_c, Z_ae, D_a. The charge density of the jth type ions $n_j(\vec{\mathbf{r}},t)$ at time t and position $\vec{\mathbf{r}}$ can be written as a sum of the mean value of the charge density $\langle n_j\rangle$ and its fluctuations $\Delta n_j(\vec{\mathbf{r}},t)$: $n_j(\vec{\mathbf{r}},t) = \langle n_j\rangle + \Delta n_j(\vec{\mathbf{r}},t)$. The equation of diffusion for the jth type ions in the field of the resultant electric potential ϕ is

$$\frac{\partial \Delta n_j(\vec{\mathbf{r}},t)}{\partial t} = D_j\nabla^2\Delta n_j(\vec{\mathbf{r}},t) + \frac{eZ_jn_jD_j}{k_BT}\nabla^2\phi(\vec{\mathbf{r}}) \qquad (1)$$

Taking into account the condition of electrical neutrality for the whole system $\sum_j Z_j\langle n_j\rangle = 0$, the Poisson equation defining ϕ can be written as

$$\Delta\phi(\vec{\mathbf{r}}) = -\frac{4\pi e}{\epsilon\epsilon_0}[Z_p\Delta n'_p(\vec{\mathbf{r}},t) + Z_a\Delta n'_a(\vec{\mathbf{r}},t) + Z_c\Delta n'_c(\vec{\mathbf{r}},t)] \qquad (2)$$

The system of eqs 1 and 2 can be linearized, disregarding terms containing the fluctuations to the second power. This procedure is justified if we take into account the process of condensation of counterions on the polyion and treat the polyion charge as an effective one z_{eff}. After linearization and Fourier transformation $[\nabla^2\Delta n'_j(\vec{\mathbf{r}},t) \rightarrow -q^2\Delta n'_j(\vec{\mathbf{q}},t)]$, we obtain

$$\frac{\partial\Delta\mathbf{n}'(\vec{\mathbf{q}},t)}{\partial t} = -\Omega(\vec{\mathbf{q}})\cdot\Delta\mathbf{n}'(\vec{\mathbf{q}},t) \qquad (3)$$

where

$$\Delta\mathbf{n}'(\vec{\mathbf{q}},t)^T = [\Delta n'_p(\vec{\mathbf{q}},t),\Delta n'_a(\vec{\mathbf{q}},t),\Delta n'_c(\vec{\mathbf{q}},t)] \qquad (4)$$

and

$$\Omega(\vec{\mathbf{q}}) = \begin{bmatrix} D_p(q^2+\lambda_p^{-2}) & \frac{D_pZ_a}{Z_p\lambda_p^2} & \frac{D_pZ_c}{Z_p\lambda_p^2} \\ \frac{D_aZ_p}{Z_a\lambda_a^2} & D_a(q^2+\lambda_a^{-2}) & \frac{D_aZ_c}{Z_a\lambda_a^2} \\ \frac{D_cZ_p}{Z_c\lambda_c^2} & \frac{D_cZ_a}{Z_c\lambda_c^2} & D_c(q^2+\lambda_c^{-2}) \end{bmatrix} \qquad (5)$$

where q is the scattering vector defined as

$$q = (4\pi n/\lambda)\sin(\theta/2) \qquad (6)$$

where n is the refractive index of the solvent, λ is the wavelength of the incident light, and θ is the observation angle of the scattered light relative to the transmitted beam, and λ_j^2 is expressed as

$$\lambda_j^{-2} = \frac{4\pi e^2}{\epsilon\epsilon_0 k_BT}\langle n_j\rangle Z_j^2 \qquad (7)$$

and corresponds to a contribution of the jth type of ions into the screening parameter of Debye−Hückel theory:

$$\frac{1}{\lambda_{DH}^2} = \lambda_a^{-2} + \lambda_p^{-2} + \lambda_c^{-2} \qquad (8)$$

The eigenvalues of the matrix $\Omega(\vec{\mathbf{q}})$, usually denoted as λ_1, λ_2, λ_3, describe the fluctuation decay time scales of three diffusion modes. λ_1 does not depend on q and describes the decay time of the charge fluctuation, while

$$\lambda_2 = D_p^{app}q^2 + A_1q^4 + A_2q^6 + ... \qquad (9)$$

$$\lambda_3 = D_s^{app}q^2 + B_1q^4 + B_2q^6 + ... \qquad (10)$$

In these equations D_p^{app} is an apparent value of the diffusion coefficient of the polyion in which the polyion coupling with small ions is taken into account, and D_s^{app} is an apparent value of the diffusion coefficient for small ions. In the limit $q \rightarrow 0$, which holds for light scattering

$$D_p^{app} = \frac{\lambda_2}{q^2} \qquad (11)$$

$$D_s^{app} = \frac{\lambda_3}{q^2} \quad (12)$$

In certain limiting cases, analytical solutions of this equation are possible, providing apparent values of the diffusion coefficients.[8−10] However, in general the apparent diffusion coefficient values are calculated numerically as the eigenvalues of the $\Omega(\vec{q})$ matrix. In the present work, the eigenvalues of this matrix were calculated numerically with the MATLAB package for given values of q, polyion, and small ion concentrations, effective charge of the polyion z_{eff}, and diffusion coefficients of the cations, anions, and polyions.

III. Experimental Methods

Material. The oligonucleotide used in this study was a synthetic single-stranded DNA 24 mer with the primary structure of human telomeric DNA d(5′-TTAGGGTTAGGGTTAGGGTTAGGG-3′). The DNA was purchased from two sources: the Midland Certified Reagent Company, Midland, Texas, and Bionovo-Bioresearch Equipment, Legnica, Poland. The sample was synthesized by the cyanoethylphosphoramide method, purified by means of HPLC, and desalted by gel filtration. The purity of the sample was typically 98%. The product was supplied from the Midland Company as the lyophilized sodium salt of DNA, and as a salt-free lyophilized DNA from Bionovo.The molecular weight is 7575 g/mol for a single-stranded DNA. The extinction coefficient used for determination of the oligonucleotide concentration at 260 nm was 29.3 μg/mL according to the information provided by suppliers.

Methods. *Dynamic Light Scattering-Photon Correlation Spectroscopy.* Samples for the PCS measurements were dissolved in 10 mM Tris HCl pH 7.3 buffer, and the final salt concentrations were adjusted by multiple dialysis. The dialyzed samples were filtered through a Millipore 0.22 μm pore size filter and centrifuged at about 8000 rotations per minute for the time from 1 to 3 h. The DNA concentration in the sample was determined by UV absorption at $\lambda = 260$ nm. The DNA concentrations in the samples subjected to PCS measurements ranged from 35 to 0.9 mg/mL, which corresponded to the molar concentrations in strands varying from 5 to 0.1 mM. The DNA concentration was decreased in a sample by dropwise addition of a certain volume of the buffer of the proper ionic strength. The ionic strength in the sample was changed by dialysis on dialyzation columns, always from low to high concentration. Prior to experiment, the samples were equilibrated at room temperature for a few hours.

The light source was an Ar^+ laser operating at $\lambda = 488$ nm with an output power of 480 mW. The vertically polarized component of scattered light was analyzed by an ALV-5000 digital correlator. The correlation functions were measured at 20 °C and at a scattering angle of $\theta = 90°$. The first 45 channels of the correlation function were analyzed, which was enough to cover the whole range of variation of the function studied. The correlation function was analyzed by the multiexponential model to obtain the relaxation times describing the translational diffusion processes τ_i and the amplitudes A_i of these processes describing their contributions to the total light scattering. The values of the translational diffusion coefficients were determined from the formula $D_T = 1/\tau q^2$, where q is the scattering vector defined by eq 6.

Circular Dichroism. CD measurements were collected on a Jasco J-715 spectropolarimeter. The DNA sample was dissolved in a buffer of 10 mM TRIS HCl of pH 7.3 and subjected to 5-fold dialysis in the buffer, heated to 95 °C, incubated at this temperature for 3 min, and then slowly cooled to 20 °C. For determination of the saturation curves, an aliquot of 2 M salt was added to the solution and the samples were equilibrated at room temperature for approximately an hour until the spectra showed no farther changes. To check this procedure some samples were equilibrated for 2 days and the spectra did not show significant changes as compared to the spectra taken after 45 min of equilibration. For determination of the melting curves, after addition of 2 M salt the sample was heated to 95 °C, incubated at this temperature for 3 min, and then cooled to 20 °C. Prior to the thermal denaturation experiments the samples were equilibrated at room temperature for a few hours. For each denaturation curve a corresponding renaturation curve was determined. The DNA concentration in the sample was determined on the basis of UV absorption at $\lambda = 260$ nm. The concentrations expressed as molar concentrations in strands varied from 1.1 to 4.4 μM.

IV. Results and Discussion

Hydrodynamic Parameters of Telomeric Structures. The possibility of occurrence of the following telomeric G-quadruplex structures was considered in this study: antiparallel monomer (Figure 1a), parallel monomer (Figure 1b), hairpin related dimmer (Figure 1c), and linear tetramer (Figure 1d).

The theoretical values of the translational diffusion coefficients for these structures were calculated on the basis of the bead model proposed by Banachowicz et al.[11] where each nucleotide was divided into two groups of atoms for consideration: the first one containing the nitrogen base and the second one the sugar and phosphate residue. Each of these groups was then replaced by a bead of a radius of $\sigma = 5$ Å, positioned at the geometric center of a given group. For the resulting system of beads the translational diffusion coefficient was numerically calculated using the algorithm proposed by Richard Pastor, taking into account the Rotne−Prager tensor of hydrodynamic interactions for partly overlapping elements.[12] For the $d(TTAGGG)_4$ sequence studied, for monomeric structures numerical calculations were performed using the atomic coordinates for monomers observed for the $d[AG_3(T_2AG_3)_3]$ sequence available from the Brookhaven Protein Data Bank modified by adding two thymines at the end of the 5′ strand, with the help of the HyperChem6 program. The translational diffusion coefficient for the antiparallel monomer (PDB access code 143d)[1], calculated on the basis of these data, was $D_T = 1.42 \times 10^{-6}$ cm^2/s, while for the parallel monomer (PDB access code 1kf1)[2] was $D_T = 1.34 \times 10^{-6}$ cm^2/s. The HyperChem6 program was used for design of the structures of dimers and tetramers of the telomeric sequence studied. The possible structures of dimers with parallel, antiparallel, and diagonal loops were considered. The translational diffusion coefficients calculated for those structures were all very similar, with D_T approximately 1.04×10^{-6} cm^2/s. The translational diffusion coefficient calculated for the tetramer was $D_T = 0.80 \times 10^{-6}$ cm^2/s.

CD Saturation Curves: The Process of Quadruplex Formation. The CD spectra of the human telomere sequence $d(TTAGGG)_4$ in the presence of the ions K^+, Na^+, Rb^+, Li^+, Cs^+, Sr^{2+}, Ca^{2+}, Mg^{2+} in different concentrations were recorded at 2 and 20 °C. The concentrations of particular salts were varied up to the values above which no spectral changes were observed. From among the ions studied, only the presence of Ca^{2+} and Mg^{2+} was not observed to stimulate the formation of any ordered structure. In the presence of the other ions, with increasing concentration a maximum at λ close to 290 nm increased in intensity, and the signal at about $\lambda = 260$ nm

TABLE 1: Thermodynamic Parameters of the Quadruplex: Random Coil Thermal Transition of d(TTAGGG)$_4$

salt	concn [mM]	λ_{max} [nm]	T_m [°C]	$\Delta H°$ [kcal/mol]	$\Delta S°$ [cal/(mol·K)]	$\Delta G°$ [a] [kcal/mol]
$SrCl_2$	0.1	301	47.6 ± 0.1	29.5 ± 0.2	92.0 ± 0.6	2.08 ± 0.02
	0.2	301	61.0 ± 0.1	27.7 ± 0.2	82.9 ± 0.6	2.98 ± 0.02
	10	301	73.2 ± 0.3	25.8 ± 0.2	74.6 ± 0.9	3.60 ± 0.05
NaCl	50	295	42.4 ± 0.2	38.8 ± 0.1	122.9 ± 0.4	2.14 ± 0.01
	100	295	50.2 ± 0.3	40.6 ± 0.1	125.5 ± 0.6	3.16 ± 0.01
	154	295	55.1 ± 0.3	42.3 ± 0.2	128.8 ± 0.6	3.87 ± 0.02
	200	295	57.7 ± 0.3	44.1 ± 0.2	133.4 ± 0.7	4.36 ± 0.02
	250	295	60.3 ± 0.3	45.4 ± 0.2	136.2 ± 0.8	4.81 ± 0.02
	303	295	62.2 ± 0.3	47.0 ± 0.2	140.2 ± 0.9	5.21 ± 0.03
KCl	10	290	44.3 ± 0.5	41.1 ± 0.3	129.5 ± 0.9	2.50 ± 0.02
	49	290	50.2 ± 0.2	46.5 ± 0.2	143.8 ± 0.6	3.63 ± 0.02
	104	290	59.0 ± 0.4	48.4 ± 0.3	145.8 ± 1.1	4.96 ± 0.04
	148	290	63.9 ± 0.4	45.7 ± 0.3	135.7 ± 1.1	5.28 ± 0.04
	190	290	66.4 ± 0.4	51.3 ± 0.3	151.1 ± 1.1	6.25 ± 0.04
	230	290	68.6 ± 0.4	51.5 ± 0.4	150.7 ± 1.3	6.57 ± 0.05
	268	290	70.0 ± 0.4	50.9 ± 0.4	148.5 ± 1.3	6.68 ± 0.05
	305	290	71.2 ± 0.4	53.2 ± 0.4	154.4 ± 1.3	7.13 ± 0.05
	340	290	72.2 ± 0.5	54.0 ± 0.4	156.3 ± 1.5	7.38 ±0.06
RbCl	10	295	26.4 ± 0.3	33.1 ± 0.4	110.3 ± 1.3	0.15 ± 0.01
	49	295	34.8 ± 0.1	37.5 ± 0.5	121.6 ± 1.9	1.20 ± 0.01
	90	295	38.5 ± 0.1	40.0 ± 0.5	127.8 ± 0.9	1.73 ± 0.01
	104	295	40.2 ± 0.1	39.8 ± 0.4	127.1 ± 1.7	1.94 ± 0.01
LiCl	10	301	23.0 ± 0.2	15.7 ± 0.3	52.8 ± 0.9	0.11 ± 0.01
	49	301	27.8 ± 0.2	26.9 ± 0.3	89.4 ± 1.0	0.25 ± 0.02
	90	301	31.2 ± 0.2	28.6 ± 0.3	93.8 ± 0.8	0.59 ± 0.01
	104	301	32.0 ± 0.2	28.6 ± 0.3	93.6 ± 0.8	0.66 ± 0.02
CsCl	180	300	27.4 ± 0.3	27.7 ± 0.6	92.1 ± 1.8	0.22 ± 0.02
	215	300	27.4 ± 0.3	27.7 ± 0.6	93.6 ± 1.8	0.22 ± 0.02
	230	300	27.7 ± 0.3	29.2 ± 0.6	98.8 ± 1.8	0.27 ± 0.02

[a] Calculated at 25 °C using eq 16. $\Delta H°$ and T_m obtained from the fit of the melting curves using eqs 14−16, and $\Delta S° = \Delta H°/T_m$. Total strand concentrations are respectively: $SrCl_2$ [DNA] = 2.0 μM, KCl [DNA] = 4.2 μM, NaCl [DNA] = 4.1 μM, RbCl [DNA] = 2.5 μM, LiCl [DNA] = 2.4 μM, CsCl [DNA] = 4.1 μM.

decreased. In consistence with the earlier study[4] the structures formed were identified as monomeric quadruplexes. For the characteristic wavelength of the quadruplex formation, see Table 1, the saturation curves were obtained. For convenience in comparing the saturation curves, the amplitude of the CD signal for the characteristic wavelength was normalized by dividing the value of the given CD signal by the DNA concentration and the path length through the measuring cell. In general, for the saturation curves obtained at 2 °C it was easier to distinguish the saturation concentration of the ions than for the curves recorded at 20 °C. Figure 2a presents the saturation curves recorded at 20 °C for all ions studied, except the curve for Li, which was obtained at 2 °C. It was impossible to observe the saturation curve for Li at 20 °C in the concentration range studied. In the presence of Cs^+ it was impossible to obtain a saturation curve at either of the two temperatures. With increasing concentration of CsCl, up to 3 mM, the CD signal at λ = 300 nm increased. This suggested formation of monomeric quadruplex; however, the presence of CsCl in higher concentrations seemed to destabilize this structure. Because the scale of the salt concentrations is logarithmic, the saturation curves are sigmoidal, and the saturation limit corresponds to the salt concentration where the value of the CD amplitude obtains half its maximum value. As shown in Figure 2a the monovalent ion concentration, for which a saturation is reached, is in the millimolar range. Distinctively the saturation limit for strontium is shifted to the micromolar range. The CD spectra for NaCl concentrations from 0 to 60 mM are presented in Figure 2b and for KCl concentrations from 0 to 4 mM in Figure 2c. For concentrations higher than the above values up to the maximum concentrations studied, 200 mM, the spectra were practically unchanged. The CD spectra for $SrCl_2$ concentrations from 0 to 42 μM are presented in Figure 2d.

With increasing salt concentration a maximum was observed to appear at λ = 295 nm in the presence of NaCl in solution, at λ = 290 nm in the presence of KCl, and at λ = 301 nm in the presence of $SrCl_2$, which is in agreement with earlier reports.[4,13] The changes in the CD spectra were interpreted as indicative of formation of the monomeric quadruplex. In the presence of NaCl two clear isoeliptic points were observed for λ of 249 and 276 nm. In the presence of KCl a less distinct isoeliptic point was noted at λ = 263 nm. In the presence of $SrCl_2$ there is no clear isoeliptic point; nevertheless, judging by the shape of the spectra they still indicate the same structural transition as for sodium and potassium. The absence of an exact isoeliptic point might be due to the presence of some third form seen in the spectra (perhaps with the maximum at around 272 nm). The other possibility is that the strontium concentration can affect the CD spectra of the given structure without substantial change of conformation. The saturation curves were obtained at 2 and 20 °C, see Figure 3a for NaCl, Figure 3b for KCl, and Figure 3c,d for $SrCl_2$. The curves were used for specification of the conditions for further measurements. It can be safely assumed that at 20 °C above the concentrations 30 mM for NaCl and 4 mM for KCl, a saturation limit is obtained. The effect of Sr^{2+} ions on the formation of monomeric quadruplex structure is exceptionally strong in comparison with that of other ions studied, and the saturation is reached already in the concentration range of micromoles as shown in Figure 3c,d. It is consistent with previous observations that Sr^{2+} is a very effective gelating agent of GMP salts.[12] Recently it also has been shown that Sr^{2+} ions strongly affect the formation of quadruplex structures by telomeric sequences of DNA.[15−19] For concentrations of $SrCl_2$ higher than 30 mM, a gradual destabilization of the monomer quadruplex was observed (Figure 2a), which is consistent with

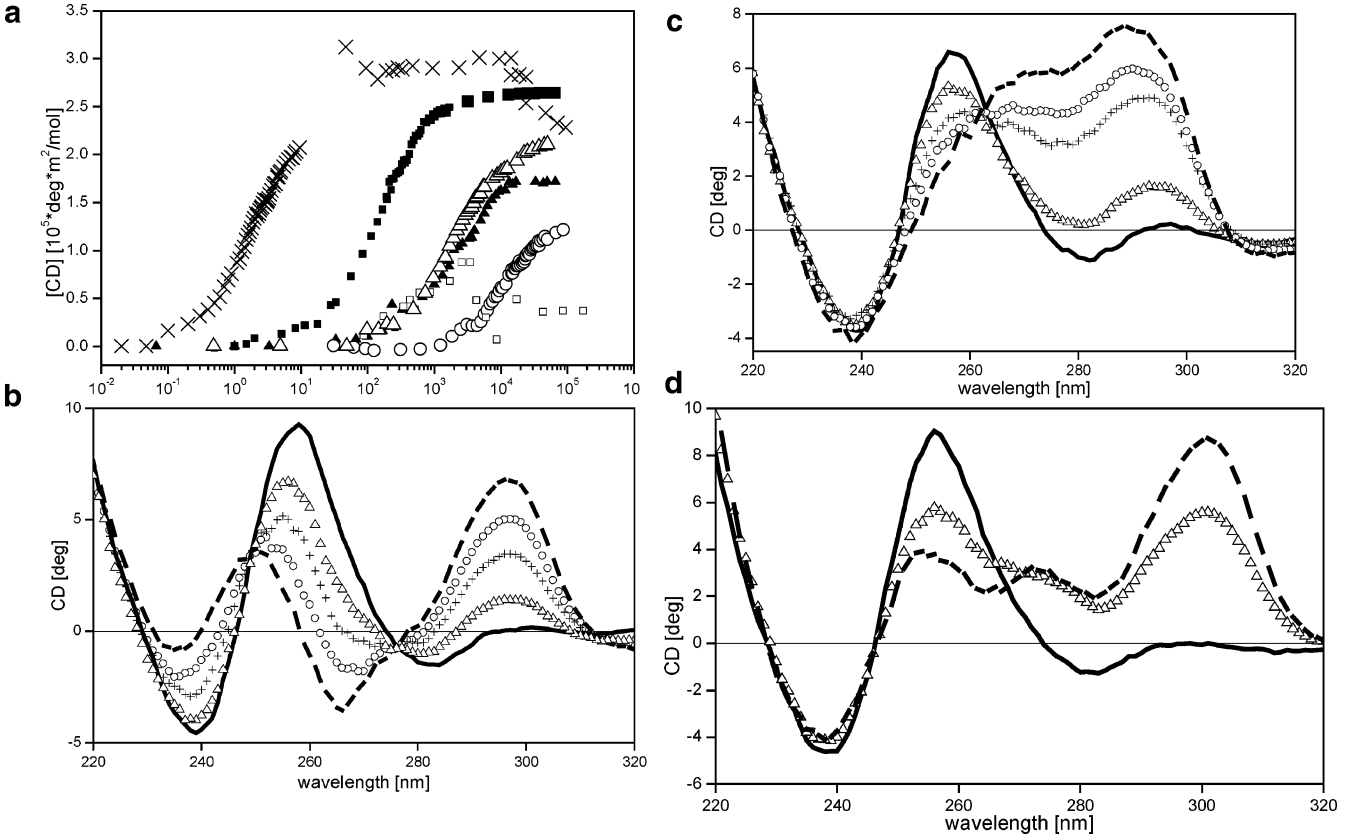

Figure 2. (a) Saturation curves recorded at 20 °C for all ions studied: K^+, Na^+, Rb^+, Cs^+, and Sr^{2+}, apart from Li^+ for which the temperature of spectra recording was 2 °C. The scale of the ratio of molar ion to DNA concentration is logarithmic. Symbols: $SrCl_2$ (×), KCl (▲), NaCl (△), RbCl (■), LiCl (○), CsCl (□). Telomere concentrations: $SrCl_2$ [DNA] = 2.1 μM, KCl [DNA] = 4.4 μM, NaCl [DNA] = 4.1 μM, RbCl [DNA] = 3.0 μM, LiCl [DNA] = 3.1 μM, CsCl [DNA] = 1.2 μM. The saturation curves were monitored at the following wavelengths: $SrCl_2$ 301 nm, KCl 290 nm, NaCl 295 nm, RbCl 295 nm, LiCl 301 nm, CsCl 300 nm. (b) CD spectra of the structure adopted by $(T_2AG_3)_4$ telomeric sequence measured in the presence of NaCl. [DNA] = 4.1 μM. Different CD spectra correspond to different NaCl concentrations starting from 0 mM NaCl (bold solid line) through 3 mM NaCl (△), 7 mM NaCl (+), 14 mM NaCl (○), to the final maximum concentration of 60 mM NaCl (dashed line). The decrease of the CD signal at 256 nm was observed simultaneously with the increase of the maximum at 256 nm. The wavelength λ = 295 nm was chosen as the best one to monitor the conformational changes of the telomeric structure upon the increase of Na^+ concentration. Two isosbestic points were observed at l = 249 nm and 276 nm. (c) CD spectra of the structure adopted by $(T_2AG_3)_4$ telomeric sequence measured in the presence of KCl. [DNA] = 3.2 μM. Different CD spectra correspond to different KCl concentrations starting from 0 mM KCl (bold solid line) through 0.1 mM KCl (△), 0.5 mM KCl (+), and 1.1 mM KCl (○), to the final maximum concentration of 4 mM KCl (dashed line). The decrease of the CD signal at 256 nm was observed simultaneously with the increase of the maximum at 290 nm. The wavelength λ = 290 nm was chosen as the best one to monitor the conformational changes of the telomeric structure upon the increase of K^+ concentration. One isosbestic point was observed at l = 263 nm. (d) CD spectra of the structure adopted by $(T_2AG_3)_4$ telomeric sequence measured in the presence of $SrCl_2$. [DNA] = 4.4 μM. Different CD spectra correspond to different $SrCl_2$ concentrations starting from 0 μM $SrCl_2$ (bold solid line) through 2 μM $SrCl_2$ (△), to the final maximum concentration of 42 μM $SrCl_2$ (dashed line). The decrease of the CD signal at 256 nm was observed simultaneously with the increase of the maximum at 301 nm. The wavelength λ = 301 nm was chosen as the best one to monitor the conformational changes of the telomeric structure upon the increase of Sr^{2+} concentration.

the earlier reports on the effect of divalent ions on the stability of structures formed by telomeric DNA sequences.[20]

Particularly interesting is the saturation curve obtained at 2 °C (Figure 3d) from which the Sr^{2+} ions concentration corresponding to the saturation can be easily read out. The same results are on the insert in Figure 3d but Sr^{2+} concentration is presented as the number of ions per DNA strand. As follows from this curve, the saturation takes place for the concentration of Sr^{2+} ions at which there is one Sr^{2+} ion per DNA strand. For the 10 times higher concentration of DNA (results not shown) the saturation limit is obtained at the same 1:1 Sr^{2+} ion per DNA strand ratio. Contrary to this, saturation curves for monovalent ions do not change under variation of DNA concentration. Saturation limit depends only on the concentration of salt. This comparison indicates that the process of monomeric quadruplex formation in the presence of Sr^{2+} has a different character than the analogous process in the presence of the other ions studied. In the presence of K^+ and Na^+ ions the process of quadruplex formation is dynamic and the ions present in the quadruplex channel can freely exchange with the ions from outside the channel.[21] The saturation curves presented in Figure 3d suggest a process in which the Sr^{2+} ion is strongly bonded at a single binding site of the telomeric DNA studied.

Photon Correlation Spectroscopy. *Results Obtained in the Presence of Na^+ Ions.* For the equilibrium concentrations of NaCl studied (50, 100, 200, 300, and 500 mM), only one diffusion mode was observed. The dependence of the translational diffusion coefficient D_T related to this mode on the DNA concentration in the presence of 50 and 100 mM NaCl is shown in Figure 4, parts a and b, respectively. In the limit of zero DNA concentration individual molecules can be approximated as noninteracting and the value D_T can be treated as that corresponding to individual molecules. In extrapolation to zero DNA concentration the values of D_T tend to a limiting value of 1.4×10^{-6} cm^2/s, which is close to D_T calculated within the bead model for the antiparallel monomer ($D_T = 1.42 \times 10^{-6}$

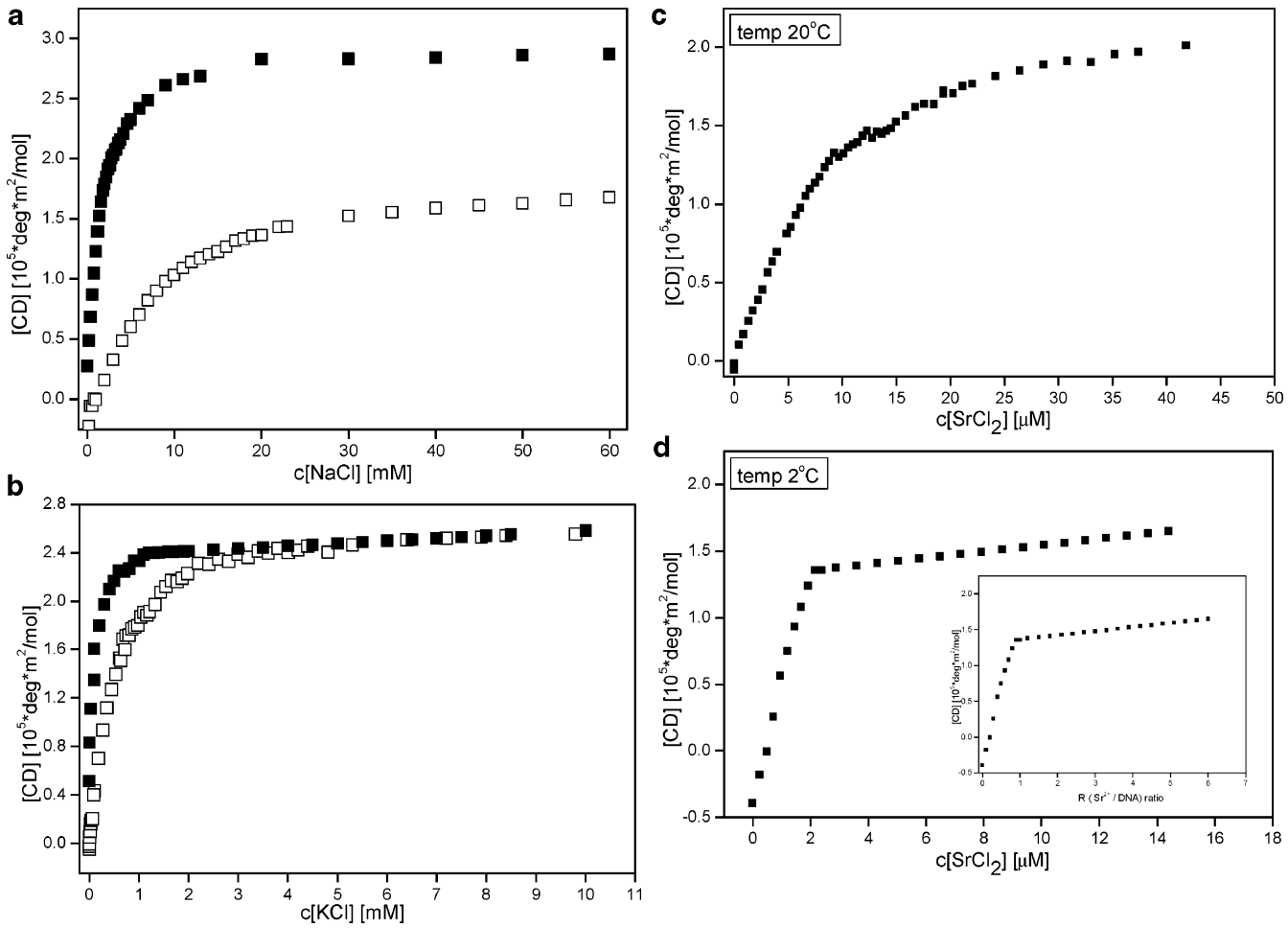

Figure 3. (a) CD saturation curves monitored at $\lambda = 295$ nm in the presence of NaCl at 20 (□) and 2 °C (■). For the experiment conducted at 20 °C [DNA] = 4.1 μM and at 2 °C [DNA] = 2.2 μM. In the case of the 20 °C experiment the saturation is obtained at about 30 mM NaCl, and for 2 °C at about 15 mM NaCl. The conformational transition is more pronounced at 2 °C. (b) CD saturation curves monitored at $\lambda = 290$ nm in the presence of KCl at 20 (□) and 2 °C (■). For the experiment conducted in both temperatures [DNA] = 4.4 μM. In the case of the 20 °C experiment the saturation is obtained at about 3 mM KCl, and for 2 °C at about 1.5 mM KCl. The conformational transition is more pronounced at 2 °C. (c) The normalized saturation curve obtained in the presence of Sr^{2+} ions at 20 °C. [DNA] = 4.4 μM. (d) The normalized saturation curve obtained in the presence of Sr^{2+} ions at 2 °C. [DNA] = 2.4 μM. The insert shows the same results where the Sr^{2+} ion concentration is presented as a ratio of the number of Sr^{2+} ions per DNA molecule.

cm^2/s) and parallel monomer species ($D_T = 1.34 \times 10^{-6}$ cm^2/s). Therefore, it was assumed that the diffusion mode observed here was related to the monomer; however, on the basis of the results obtained it was impossible to conclude about the conformations of monomers in solution. Because DNA molecules in solution of neutral pH are strongly charged polyions, electrostatic forces play the dominant role in the intermolecular interactions. The behavior of the collective diffusion mode in the presence of strong electrostatic interactions is described in terms of the coupled mode theory. Parts a and b of Figure 4 present the values of collective coefficients of translational diffusion calculated on the basis of this theory for different effective charges z_{eff} of the molecule, and for D_T for an individual molecule equals 1.4×10^{-6} cm^2/s. The curves calculated for the $z_{eff} = -5$ model the experimental data well; however, the curves for $z_{eff} = -6$ and -4 also provide reasonable bounds to the data set. We thus conclude that the value of $z_{eff} = -5 \pm 1$. The dependence of D_T on the concentration of NaCl is shown in Figure 4c. For high concentrations of NaCl at which the electrostatic interactions between the DNA molecules are screened, the collective coefficient of translational diffusion tends to the value for an individual molecule. In Figure 4c the horizontal lines correspond to the D_T values calculated for the parallel and anti-parallel monomer isolated species. We also show the experimentally extrapolated value of D_T in the limit of low DNA concentration (1.4×10^{-6} cm^2/s).

In the limit of high concentrations of NaCl, the value of D_T tends to 1.4×10^{-6} cm^2/s, except for one D_T value at NaCl concentration of 0.5 M, which might suggest a slightly lower limiting value. These results do not permit any conclusions about the monomer conformation, so we cannot exclude that either or both monomer forms are present in the solution. Figure 4c also presents the values of D_T calculated on the basis of the coupled mode theory. As mentioned above, the curves calculated for $z_{eff} = -4$, $z_{eff} = -5$, and $z_{eff} = -6$ all bracket the experimental results, indicating that the effective charge is $z_{eff} = -5 \pm 1$. This value is in excellent agreement with that estimated for antiparallel monomer and parallel monomer obtained on the basis of Manning theory of counterion condensation ($z_{eff} = 5.1$: see below).[22]

The antiparallel monomer structure deposited at the Protein Data Base under the access code 143d and modified by adding two thymines at the end of the 5′ strand is approximately a cylinder 2.46 nm in diameter and 3.61 nm in height. In a neutral solution this structure has 24 negatively charged phosphate

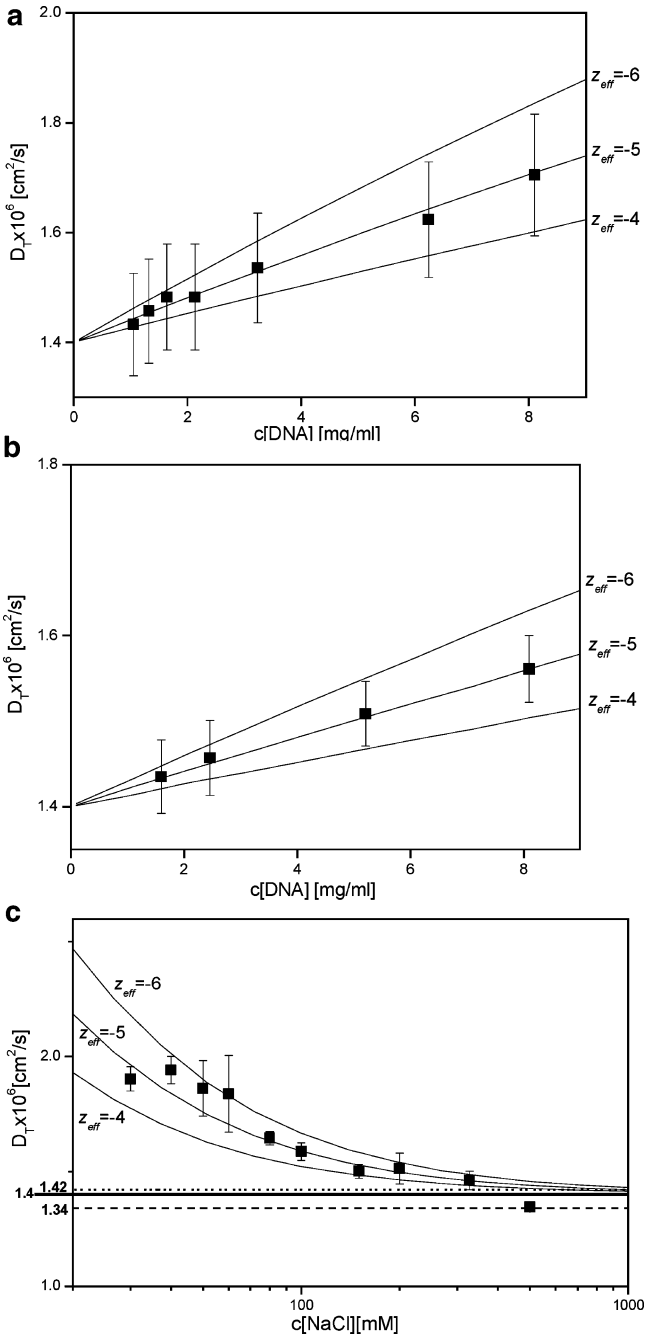

Figure 4. (a) The measured translational diffusion coefficient D_T of the diffusion mode versus the telomere concentration at [NaCl] = 50 mM. Additionally, curves generated on the basis of the coupled mode theory for the effective charges $z_{eff} = -6, -5, -4$ are presented. (b) The measured translational diffusion coefficient D_T of the diffusion mode versus the telomere concentration at [NaCl] = 100 mM. Additionally, curves generated on the basis of the coupled mode theory for the effective charges $z_{eff} = -6, -5, -4$ are presented. (c) The measured translational diffusion coefficient D_T of the diffusion mode versus NaCl concentration. Curves generated on the basis of the coupled mode theory for the effective charges $z_{eff} = -6, -5, -4$ are presented. Additionally, the horizontal lines correspond to the D_T values calculated for isolated species: the parallel monomer, 1.42×10^{-6} cm^2/s (dashed line) and anti-parallel monomer, 1.34×10^{-6} cm^2/s (dotted line). The experimentally extrapolated value of D_T in the limit of low DNA concentration, 1.4×10^{-6} cm^2/s (bold solid line) is also presented. [DNA] = 9.5 mg/mL.

groups distributed over the cylinder surface in such a way that the molecule has approximately axial symmetry. For the molecule length L measured along the axis, for a molecular charge of $z = -24$ the Manning parameter $\xi_M = 4.7$, which means that a process of ion condensation will take place. The metal ions bound in the quadruplex channel change the charge of the molecule but it would take more than 19 Na^+ or K^+ ions in a channel to reduce the Manning parameter to the critical value. Since the number of the binding sites in the quadruplex channel estimated on the basis of its structure is 2 for potassium and 3 for sodium, it is reasonable to assume that condensation of the counterions on the antiparallel monomer structure will take place irrespective of the number of ions bound in the channel. Assuming that at 20 °C, $\lambda_B = 0.7115$ nm, the effective charge after condensation calculated from the formula

$$|z_{eff}| = \frac{L}{z_c \lambda_B} \tag{13}$$

is $z_{eff} = -5.1$, where z_c stands for the counterion valency. It should be emphasized that the effective charge does not depend on the number of ions bound in the channel. Corrections to Manning theory following from the finite length and radius of the molecule were applied by, e.g., Ramanathan and Woodbury;[23] however, they are not significant for polyions of length L comparable to or greater than the Debye−Hückel length λ_{DH}. In our PCS experiment the minimum concentration of NaCl was 50 mM, which corresponds to the Debye−Hückel length $\lambda_{DH} = 1.362$ nm at 20 °C. Since λ_{DH} decreases with increasing number of ions in solution, for higher concentrations the values of λ_{DH} will be even smaller, which means that in the experimental conditions used, corrections to Manning theory should not be significant.

The parallel monomer structure deposited at PDB under the access code 1kf1[2] modified by addition of two thymines at the end of the 5′ strand has a complex propeller-like shape, which has approximately four-fold symmetry about the quadruplex axis. However, its morphology is far from rod-like, so that an estimation of its effective charge on the basis of Manning theory is very problematic. In fact it is only possible to conclude that the absolute value of the effective charge on the parallel monomer will be lower than that on the antiparallel monomer, because the length of the parallel monomer measured along the quadruplex channel is much shorter than that of the antiparallel monomer. However, on the basis of the results reported by Wang and Patel[1] in the presence of Na^+ ions in solution, it can be assumed that the antiparallel monomer is dominant. The effective charge estimated on the basis of the experimental data is thus in good agreement with the conclusions following from Manning theory for the antiparallel monomer structure.

Results Obtained in the Presence of K^+ Ions. The results obtained in the presence of KCl are similar to those obtained in the presence of NaCl. In the range of all equilibrium concentrations of KCl (4, 6, 8, 10, 15, 20, 30, 50, 100, 200, 300, 500 mM) only one diffusion mode was observed. Measurements of D_T related to this mode as a function of DNA concentration in the presence of 10 and 50 mM KCl are shown in Figure 5, parts a and b, respectively. The values of D_T extrapolated to zero DNA concentration tend to 1.4×10^{-6} cm^2/s, which permits us to assume that the diffusion mode corresponds to monomers. The curves calculated on the basis of the coupled mode theory for $z_{eff} = -3$, -4, and -5 bracket the experimental data and give the effective charge as $z_{eff} = -4 \pm 1$. The dependence of D_T on KCl concentration is shown in Figure 5c.

In the limit of high KCl concentrations the value of D_T is close to 1.4×10^{-6} cm^2/s, although at the KCl concentration of 0.5 M the value of D_T is even lower than 1.34×10^{-6} cm^2/

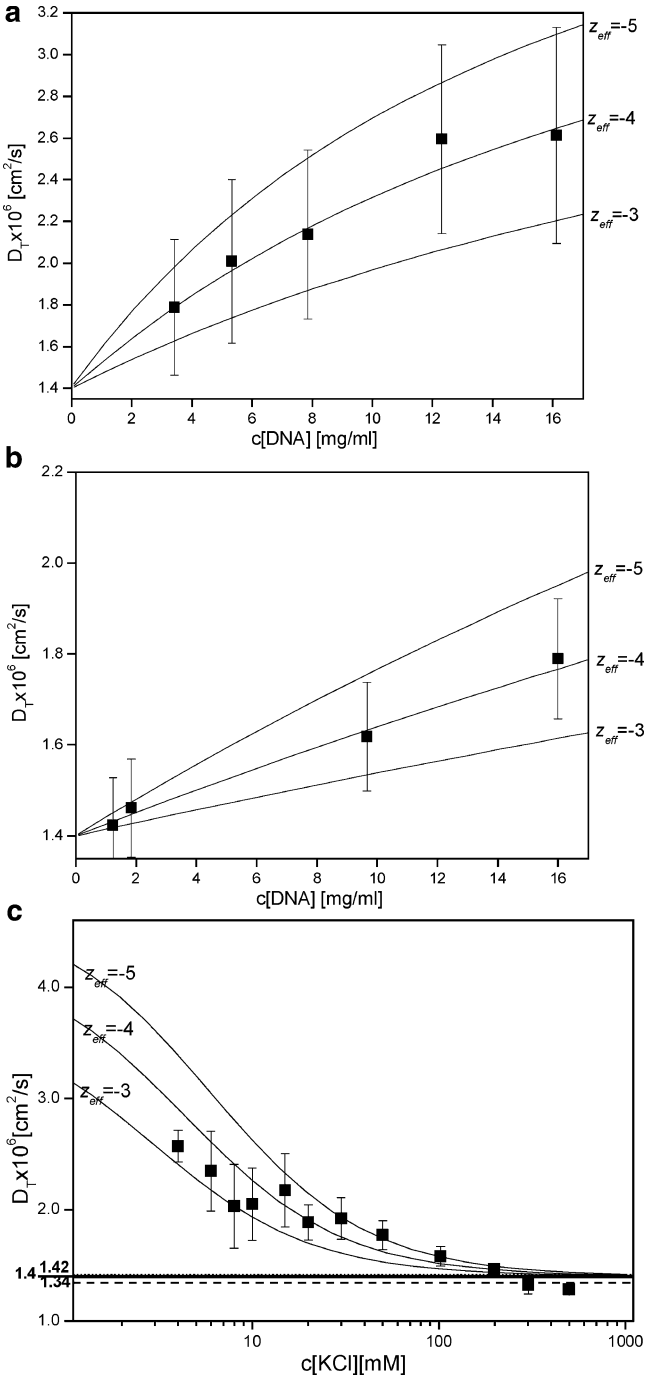

Figure 5. (a) The measured translational diffusion coefficient D_T of the diffusion mode versus the telomere concentration at [KCl] = 10mM. Additionally, curves generated on the basis of the coupled mode theory for the effective charges $z_{eff} = -5, -4, -3$ are presented. (b) The measured translational diffusion coefficient D_T of the diffusion mode versus the telomere concentration at [KCl] = 50 mM. Additionally, curves generated on the basis of the coupled mode theory for the effective charges $z_{eff} = -5, -4, -3$ are presented. (c) The measured translational diffusion coefficient D_T of the diffusion mode versus KCl concentration. Curves generated on the basis of the coupled mode theory for the effective charges $z_{eff} = -5, -4, -3$ are presented. Additionally, the horizontal lines correspond to the D_T values calculated for isolated species: the parallel monomer, 1.42×10^{-6} cm^2/s (dashed line), and anti-parallel monomer, 1.34×10^{-6} cm^2/s (dotted line). The experimentally extrapolated value of D_T in the limit of low DNA concentration, 1.4×10^{-6} cm^2/s (bold solid line), is also presented. [DNA] = 9.2 mg/mL.

s, which is the value corresponding to the parallel monomer. The results do not permit drawing definitive conclusions on the monomer conformation; however, D_T obtained at 0.5 M concentration of KCl suggests the presence of parallel monomer in solution. Figure 5c presents also the results of the coupled mode theory calculations. The curves calculated for $z_{eff} = -3$, -4, and -5 again agree with the experimental results, allowing an estimation of the effective charge as $z_{eff} = -4 \pm 1$. The effective charge estimated for the antiparallel monomer in the presence of K^+ ions on the basis of Manning's theory of counterion condensation is $z_{eff} = -5.1$, similar as in the presence of Na^+ ions. The only difference is that some of the K^+ ion concentrations studied were significantly lower that those of Na^+ ions. For the lowest KCl concentrations of 1, 4, 6, and 8 mM some corrections for the molecular size should be included in Manning theory; however, for such low concentrations, the effective charge was not experimentally determined. As in the case of Na^+ described above the effective charge determined from analysis of experimental results obtained in the presence of K^+ agrees well with the approximate estimations based on Manning theory, for the antiparallel monomer. As before, it is impossible to discern which form of the monomer is present in solution, as the effective charge of the parallel monomer is not known theoretically. However, it does appear that a lower effective charge is obtained in the presence of KCl than for NaCl, and this could suggest the presence of the parallel monomer in KCl solution.

Results Obtained in the Presence of Sr^{2+} Ions. In the presence of $SrCl_2$ at the concentrations 1 and 15 mM, the sample was polydisperse. In the presence of 1 mM $SrCl_2$, PSC data indicated two diffusion modes. The values of the translational diffusion coefficients D_T corresponding to these modes versus the DNA concentration do not change. The theoretical D_T values were compared with the experimental values extrapolated to the limit of zero DNA concentration (noninteracting particles). The values of D_T extrapolated to zero DNA concentration tend to 1.4×10^{-6} cm^2/s for one mode and to 6.2×10^{-8} cm^2/s for the other. The value 1.4×10^{-6} cm^2/s is close to those obtained theoretically for monomeric antiparallel $D_T = 1.42 \times 10^{-6}$ cm^2/s and parallel $D_T = 1.34 \times 10^{-6}$ cm^2/s quadruplexes. Therefore, we assumed that the first of the diffusion modes corresponds to the monomeric quadruplexes. Again, the experimental results do not permit a differentiation between these two monomeric forms in solution. The translational diffusion coefficient of the second diffusion mode is on the order of 10^{-8} cm^2/s, which suggests a large size and mass of the scattering objects corresponding to this mode; these objects are henceforth referred to as aggregates 1. On the basis of the diffusion coefficient of aggregate 1 extrapolated to zero DNA concentration, which equals 6.2×10^{-8} cm^2/s, it is possible to estimate that this aggregate has hydrodynamic radius $\sigma = 345$ Å, and its mass as 12500 of monomer masses. As follows from the results of the relative amplitudes of the diffusion modes corresponding to the monomer and aggregate 1, the relative weight concentration of the monomer is equal to 1 and that of the aggregate 1 is close to zero. Its presence is detected thanks to the particularly high sensitivity of the PCS method to the signals from large structures.

In the presence of $SrCl_2$ in the concentration of 15 mM, three diffusion modes were detected. Figure 6a presents the dependence of D_T values assigned to these modes on DNA concentration. The values of D_T assigned to these modes extrapolated to zero DNA concentration were 1.4×10^{-6}, 0.8×10^{-6}, and 0.2×10^{-6} cm^2/s. The diffusion mode described by the D_T value of 1.4×10^{-6} cm^2/s was assigned to monomeric quadruplexes. The value of D_T corresponding to the second mode extrapolated

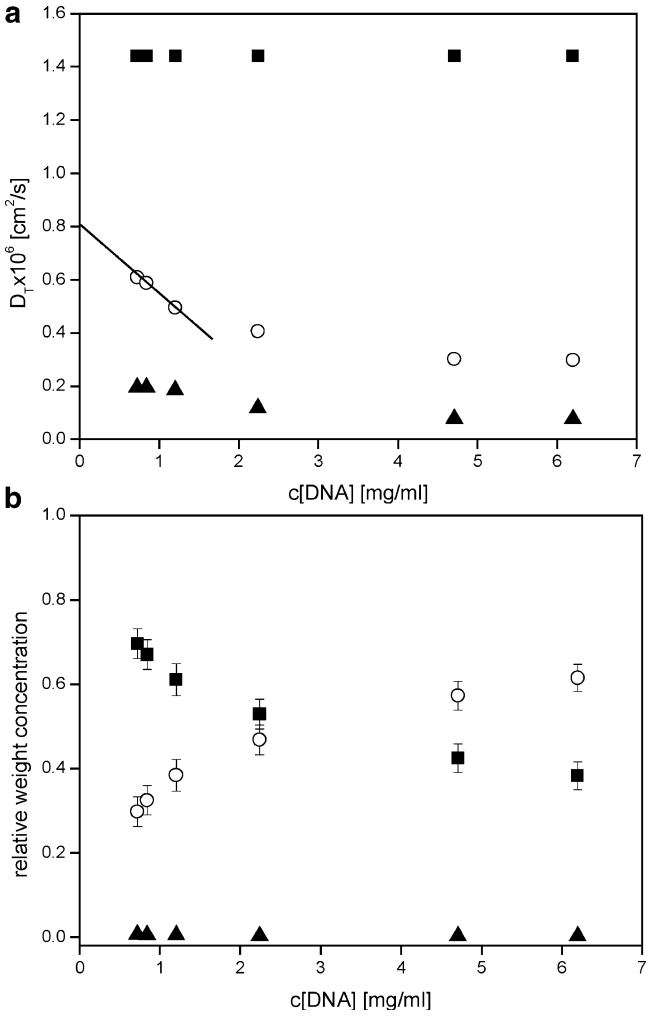

Figure 6. (a) The measured translational diffusion coefficient of the three forms of the telomere versus the telomere concentration at 15 mM $SrCl_2$. Symbols: (▲) monomer, (○) tetramer, (■) aggregate 2. The errors where smaller than the size of the symbols indicating experimental points. (b) Relative weight concentrations of the monomer (▲), tetramer (○), and agregat 2 (■) versus the telomere concentration at 15 mM $SrCl_2$.

to zero DNA concentration equals 0.8×10^{-6} cm^2/s. This is the same value as that theoretically calculated for a linear tetramer; therefore, this structure was assumed as corresponding to this value of D_T. Because the values of D_T for monomeric quadruplex and tetramer were quite close it was difficult to fit the multiexponential model to the results in the low DNA concentration limit where the PCS signal from small structures was weaker. Therefore the value of D_T for the monomeric DNA was fixed for the three points with the lowest DNA concentration. Assumption of a constant value of D_T for a monomer in the low DNA concentration limit is justified by earlier results in 1 mM SrCl2 where no D_T dependence on DNA concentration was observed for a monomeric quadruplex. Contrary to the behavior of D_T for monomeric quadruplex the values of D_T for a tetramer have shown substantial dependence on the DNA concentration. In the limit of low DNA concentration one assumes linear dependence of D_T versus DNA concentration. Clearly the values of D_T assigned to a tetramer do not follow linear dependence in the whole range of DNA concentration studied. Therefore for the D_T extrapolation to zero DNA concentration limit we have used only three points corresponding to the lowest DNA concentration studied.

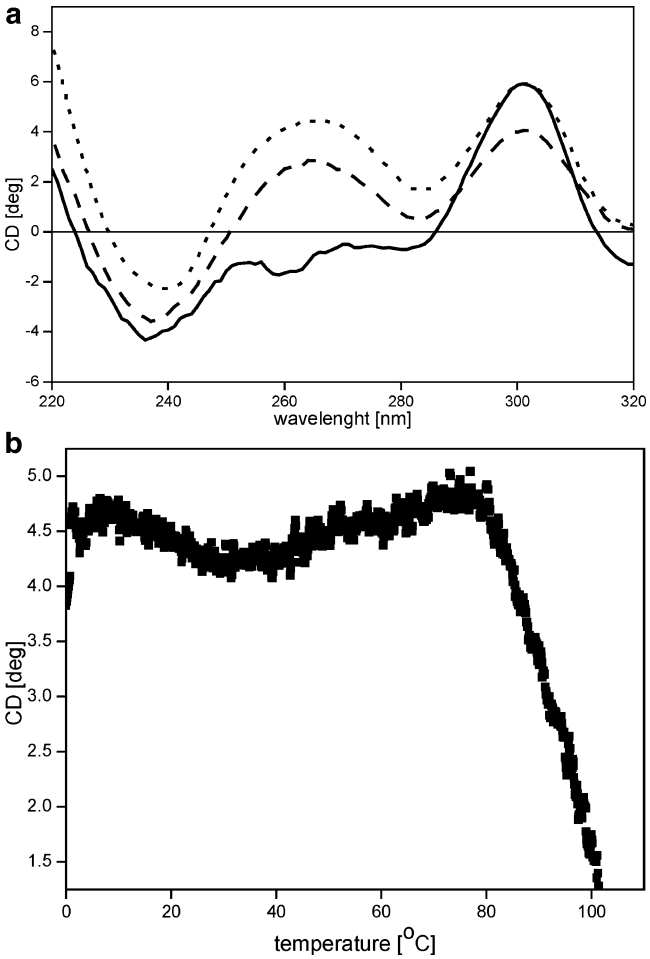

Figure 7. (a) The CD spectra recorded in the presence of 50 mM $SrCl_2$ at 20 °C before the thermal denaturation (solid line), after the denaturation and renaturation (dashed line), and after a 2-day incubation at 20 °C after denaturation and renaturation (dotted line). [DNA] = 2.0 μM. (b) CD melting curve of the tetramere at 50 mM $SrCl_2$ recorded at λ = 260 nm. [DNA] = 2.0 μM.

On the basis of the value of D_T corresponding to the third mode equal to 0.2×10^{-6} cm^2/s, it was possible to estimate the size of the structure it described as σ = 100 Å and its mass as 300 of the monomer masses. This structure was referred to as aggregate 2. Figure 6b presents relative weight concentrations of monomeric quadruplex, tetramer quadruplex, and aggregate 2 obtained from analysis of relative amplitudes of the diffusion modes corresponding to these structures. The results indicate that the weight concentration of aggregate 2 is close to zero in the whole DNA concentration range studied. The data shown in Figure 6b also imply that for DNA concentrations lower than 2 mg/mL, the structure dominating in solution is the monomeric quadruplex. With increasing concentration of DNA the formation of tetrameric quadruplex becomes favored, so for DNA concentrations higher than 5 mg/mL, the dominant structure is the tetrameric quadruplex. The conformational transition monomer-tetramer takes place for DNA concentrations from 2.2 to 4.8 mg/mL. The formation of tetramer observed with increasing DNA concentration is a manifestation of a general tendency toward formation of multistranded telomeric structures in the presence of DNA in higher concentrations.[24−26]

The analysis of CD spectra indicated formation of the tetrameric quadruplex structure in the presence of $SrCl_2$ concentration of 50 mM and only after thermal denaturation and renaturation of the sample (Figure 7a,b). However, compar-

ing the CD results with PCS results it must be regarded that the CD spectra were taken for samples of much lower DNA concentrations. In the samples for CD measurements the DNA concentrations were of the order of micromoles per liter, while in the samples for PCS measurements the order was millimoles per liter, thus a thousand times higher. According to the data in Figure 6b, the concentration of tetramer rapidly decreases with decreasing DNA concentration, so in the CD spectra taken in the presence of 15 mM of $SrCl_2$ there are no signals assigned to tetramers.

Thermal Denaturation Curve Analysis. The melting curves of the telomeric sequence $d(TTAGGG)_4$ were recorded by the CD method. The CD signal was recorded at the same wavelengths at which the saturation curves were studied; examples are shown in Figure 8a,b,c.

The curves recorded in the presence of all ions studied (K^+, Na^+, Rb^+, Li^+, Cs^+, Sr^{2+}) at all concentrations indicated a well-defined cooperative melting process. The van't Hoff thermodynamic parameters describing the transition quadruplex-random coil and the melting temperatures of the monomer quadruplex structure were determined by parametrization of the melting curves using the two state van't Hoff model.[27−29] The functions used to fit the melting curves are

$$\alpha = \frac{K(T)}{1 + K(T)} \tag{14}$$

$$K(T) = \exp\left(-\frac{\Delta G^\circ}{RT}\right) \tag{15}$$

$$\Delta G^\circ = \Delta H^\circ\left(1 - \frac{T}{T_m}\right) \tag{16}$$

where α is the fraction of the folded quadruplex, $K(T)$ is the equilibrium constant, T_m is the melting temperature, ΔG° is the Gibbs free energy change, and ΔH° is the enthalpy change. Obtained thermodynamic parameters of the quadruplex-random coil thermal transition are presented in Table 1. The results presented in Table 1 and Figure 2a imply the following ordering of the ions studied according to the efficiency of the formation of monomeric quadruplex structures and their stabilization: $Sr^{2+} > K^+ > Na^+ \geq Rb^+ > Li^+ > Cs^+$. Similar conclusions have been formulated for other telomeric sequences.[12]

Results Obtained in the Presence of Na^+ and K^+ Ions. In the DNA range studied (2 −8 μM) T_m is constant in the presence of Na^+ and K^+, which confirms that the melting curves observed correspond to monomeric structures. The dependencies of T_m and ΔG° on the logarithm of the ion concentrations are shown in Figure 9, parts a and b, respectively. Both dependencies are linear, which permits determination of the number of ions released upon unfolding.

Assuming a simple model involving an all-or-none transition from ordered quadruplex to random coil:

$$\text{quadruplex} \rightarrow \text{random coil} + \Delta n \tag{17}$$

where Δn is the number of ions released upon transition that can be found from the formula[30]

$$\Delta n = 2\frac{1}{RT}\frac{\partial \ln \Delta G^\circ}{\partial \ln[M]} \tag{18}$$

In the above formula the factor 2 comes from the Debye−Hückel screening of the DNA polyions by low molecular weight ions.[31] The values of Δn obtained from eq 18 are 5.8 ± 0.2 for quadruplex melting in the presence of NaCl and 6.6 ± 0.6 in the presence of KCl.

In eq 17 the reference states for polyions in the form of quadruplexes and random coils contain associated condensed

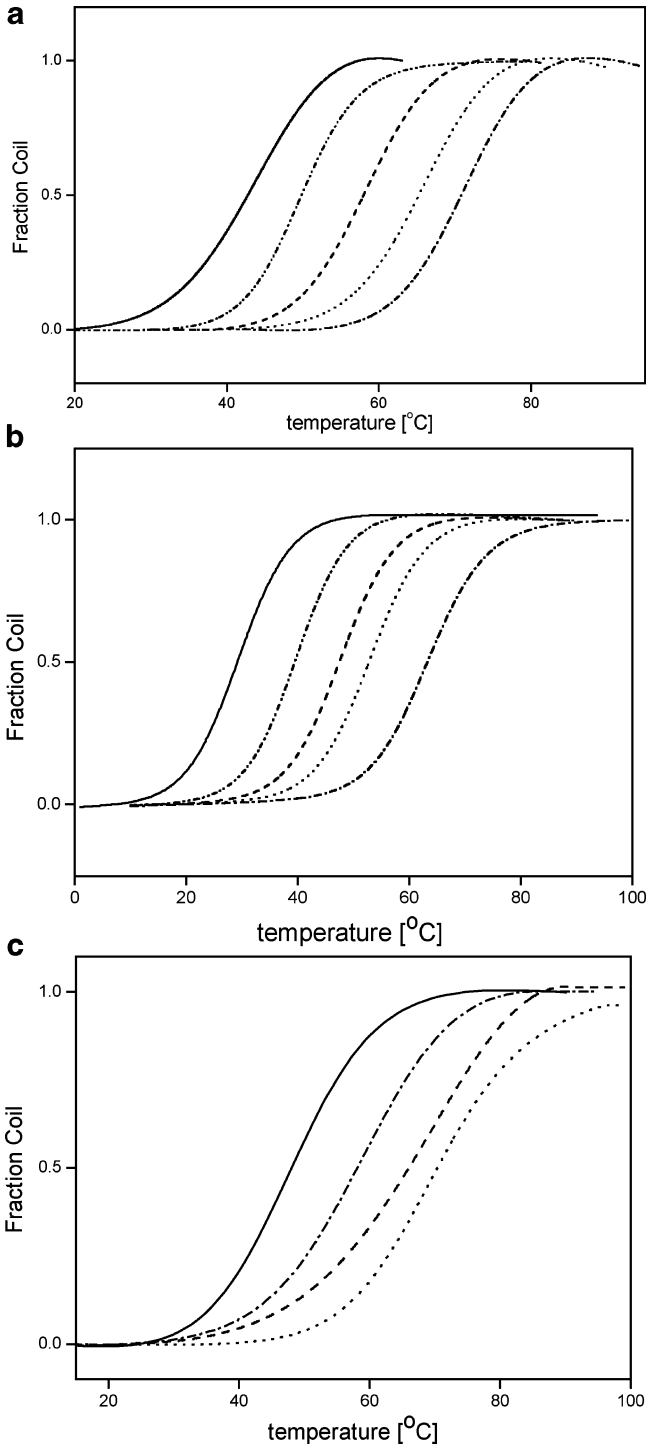

Figure 8. (a) Examples of CD melting curves obtained in the presence of KCl: 10 mM (solid line), 49 mM (dash-dot-dot line), 104 mM (dashed line), 190 mM (dotted line), 340 mM (dash−dot line). Spectra were recorded at $\lambda = 290$ nm. [DNA] = 2.8 μM. (b) Examples of CD melting curves obtained in the presence of NaCl: 10 mM (solid line), 49 mM (dash-dot-dot line), 104 mM (dashed line), 148 mM (dotted line), 340 mM (dash-dot line). Spectra were recorded at $\lambda = 295$ nm. [DNA] = 2.4 μM. (c) CD melting curves obtained in the presence of $SrCl_2$: 0.1 mM (solid line), 0.2 mM (dash-dot line), 10 mM (dashed line), 50 mM (dotted line). Spectra were recorded at $\lambda = 301$ nm. [DNA] = 2.0 μM.

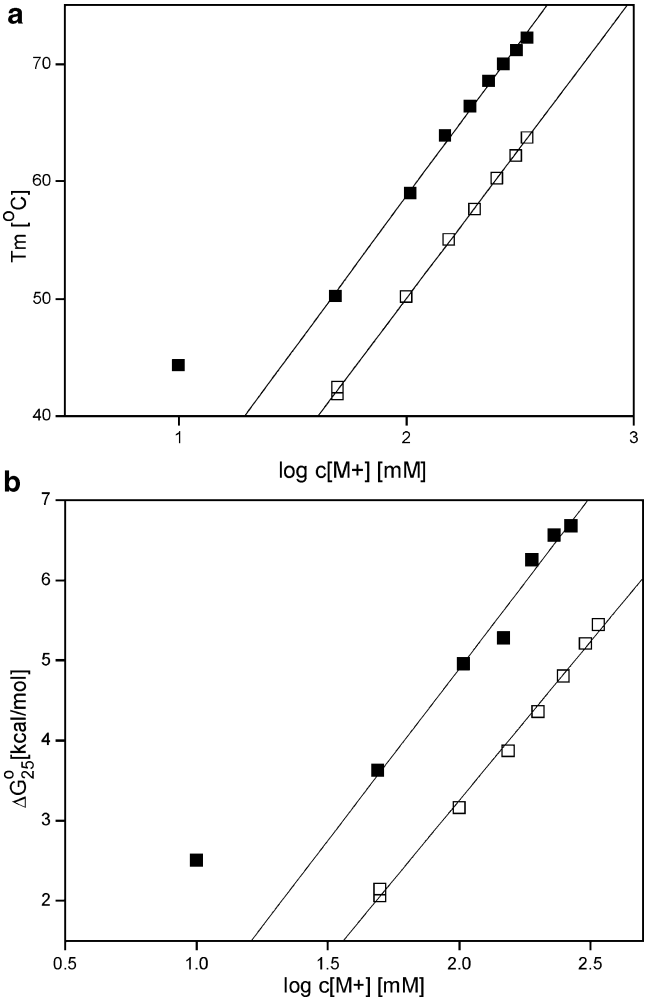

Figure 9. (a) The dependence of the melting temperatures T_m of the quadruplex structure versus Na^+ (□), and K^+ (■) concentrations. The ionic concentration is presented in a logarithmic scale. The melting temperature exhibits a linear dependence on the logarithm of the ionic concentration except for one point at 10 mM K^+. (b) The dependence of the change of the Gibbs free energy change $\Delta G_{25}°$ associated with the melting process of the quadruplex structure versus the Na^+ (□), and K^+ (■) concentrations. The ionic concentration is presented in a logarithmic scale. $\Delta G°$ exhibits a linear dependence on the logarithm of the ionic concentration (eq 18) except for one point at 10 mM K^+.

counterions, and for the quadruplex case, counterions bound in the channel. That is why the value of Δn can be determined as a difference between the effective charge on the quadruplex and that on the random coil. To estimate the effective charge of the random coil in terms of Manning theory of the counterion condensation, the length L in eq 13 should be measured along the strand.[27] Because of the richness of the purine bases in the strand studied it was assumed that a good model to study its behavior could be a denatured polyA strand. We should note that a denatured polyA strand is more condensed than a typical denatured DNA, owing to the nitrogen base stacking. The distance between the nucleotides in a denatured polyA strand is 0.31 nm, while in a typical denatured DNA it is 0.43 nm.[30] It is known that a similar nitrogen base stacking appears also in guanines. Taking into account the above considerations, the length of the random coil formed by the sequence $d(TTAGGG)_4$ has been estimated as $(24-1) \times 0.31$ nm $= 7.13$ nm, which for 24 negatively charged phosphate groups gives the Manning parameter $\xi_M = 2.4$. The condensation of polyions, according to eq 13, leads to an effective charge $z_{eff} = -10.0$. As the effective charge estimated from the experimental data for the monomer structures is $z_{eff} = -5 \pm 1$ in the presence of NaCl and $z_{eff} = -4 \pm 1$ in the presence of KCl, the number of released ions can be estimated as $\Delta n = 5 \pm 1$ in the presence of NaCl and $\Delta n = 6 \pm 1$ in the presence of KCl. These results are consistent with those obtained from the analysis of the $\Delta G°$ dependence on the logarithm of the ionic concentration described by eq 18.

The number of ions released on thermal denaturation Δn includes the ions bound in the quadruplex channel, and the difference between the number of ions condensed on the quadruplex and on the random coil. Therefore, the value of Δn is not interpreted as the number of ions bound in the quadruplex channel, as was done previously.[32] According to Manning theory the effective charge does not depend on the number of ions bound in the quadruplex channel, Δn will also be independent of that number. Therefore, in the range of applicability of Manning theory, the phenomenon of ion condensation will prevent drawing further conclusions about the number of ions bound in the quadruplex channel, on the basis of the number of released ions Δn.

Results Obtained in the Presence of Sr^{2+} Ions. The thermal denaturation process in the presence of 50 mM $SrCl_2$ was studied (Figure 8c) and it was found that the renaturation curve did not coincide with the denaturation curve. The CD spectra recorded in the presence of 50 mM $SrCl_2$ at 20 °C before the thermal denaturation, after the denaturation and renaturation, and after a 2-day incubation at 20 °C after denaturation and renaturation are shown in Figure 7a. After the cycle of denaturation and renaturation an additional maximum appeared in the CD spectra at about 260 nm, which was interpreted as the formation of a new structure. After a 2-day incubation the CD signal at about 260 nm increased, which might indicate that the process of formation of this new structure was characterized by a very slow kinetics. The melting curve of this new structure recorded at 260 nm is shown in Figure 7b and proves that the melting process is well-defined so the new structure is ordered. The melting curve could not be normalized as the process of melting did not stop even at 100 °C. The appearance of the maximum at 260 nm in the CD spectrum, high melting point, and very slow kinetics of formation of this new structure suggest the formation of tetramer quadruplex, and this interpretation has been assumed throughout this work. The formation of tetramer quadruplexes as a result of a cycle of thermal denaturation and renaturation is in agreement with earlier reports indicating that repeated cycles of denaturation and renaturation shift the equilibrium in solution toward multistranded forms.[15,33] Finally, it can be concluded that in the presence of 50 mM $SrCl_2$ and 2 μmol DNA a possibility of the existence of different equilibrium states between the monomer and tetramer quadruplex forms was observed, depending, among other things, on the history of the sample.

V. Conclusions

The influence of ions K^+, Na^+, Rb^+, Li^+, Cs^+, Sr^{2+}, Ca^{2+}, and Mg^{2+} on the formation of human telomere sequence $d(5'\text{-}TTAGGG\text{-}3')_4$ structures, their stability, and dynamics were investigated by PCS and CD methods for a wide range of concentrations of ions and DNA. The increase of the concentration of monovalent ions and Sr^{2+} resulted in a transition from the random coil to ordered structure. The ordered structure was identified as a quadruplex based on the comparison of the measured translational diffusion coefficient with calculated values based on the "bead-modeling" approach.

The PCS results obtained in the presence of Na^+ and K^+ indicated the presence of only one collective diffusion mode,

which allowed detailed analysis of intermolecular interactions. The translational diffusion coefficient of the molecules corresponding to the diffusion mode observed was $D_T = 1.4 \times 10^{-6}$ cm^2/s in the presence of Na^+ and K^+ ions. Comparison of those values with calculated results based on the bead model allowed identification of the molecules corresponding to the diffusion mode as the monomeric quadruplexes. The results did not permit differentiation between the parallel or antiparallel monomer species. The concentrations of DNA and salt significantly affected the values of D_T corresponding to the diffusion mode observed, which indicated strong intermolecular interactions. Under the conditions studied the electrostatic interactions were dominant, so the behavior of the molecules in solution was analyzed via the coupled mode theory based on the Debye−Hückel approach supplemented with the Manning theory of condensation. Curves obtained using this theory were in good agreement with the experimental results, and they allowed estimation of the effective charge of the monomeric quadruplex as $z_{eff} = -5 \pm 1$ in the presence of NaCl, and $z_{eff} = -4 \pm 1$ in the presence of KCl. These results are also in agreement with the effective charge calculated on the basis of Manning theory. The number of ions Δn released upon thermal denaturation of a quadruplex was calculated on the basis of the experimental estimations of the effective charges on the quadruplex structure. The value of Δn was also obtained by analyzing CD melting curves, in particular the thermodynamics of the thermal transition quadruplex-random coil. The analysis took into account corrections due to the electrostatic interactions. Results obtained by the two methods were in good agreement.

Analysis of the CD saturation and melting curves proved that the effect of Sr^{2+} ions on formation of monomeric quadruplexes was the greatest from among those of the ions studied (K^+, Na^+, Rb^+, Li^+, Cs^+, Sr^{2+}, Ca^{2+}, Mg^{2+}). Analysis of the saturation curve recorded at 2 °C suggested that the presence of a single Sr^{2+} ion was enough for the sequence studied to form the monomeric quadruplex structure. In the presence of 50 mM $SrCl_2$, after the sample had been subjected to thermal denaturation and renaturation, the formation of tetrameric quadruplexes was observed. PCS results permitted determination of the translational diffusion coefficients assigned to the collective diffusion modes of the structures observed in the presence of Sr^{2+}. One of the modes was assigned to monomeric quadruplexes on the basis of a comparison between the experimental D_T with the values calculated assuming the bead model. In the presence of $SrCl_2$ at a concentration of 15 mM, a mode corresponding to tetrameric quadruplexes was also detected. Besides these structures, the formation of aggregates was also observed, and their size and masses were estimated. The relative weight concentrations of these structures were determined as a function of DNA concentration. The relative weight concentrations of the aggregates were found to be close to zero. With decreasing DNA concentration a conformational transition tetramer-monomer was observed. The effect of Sr^{2+} ions on the structures formed by the human telomere sequence $d(TTAGGG)_4$ was found to be much stronger and of different character than that of the ions K^+ and Na^+. Similar conclusions were formulated on the basis of the study reported in which the PCS method was used to identify the structures made by the telomeric DNA of *Tetrahymena thermophila* $d(TGGGGT)_4$.[18,19]

Acknowledgment. A. Włodarczyk thanks Prof. J. Otlewski and Dr. D. Krowarsch from the Laboratory of Protein Engineering, Institute of Biochemistry and Molecular Biology (University of Wrocław, Poland) for allowing her to use the laboratory facilities to carry out the CD experiments and for the valuable discussions. A. Włodarczyk is currently supported by a Wolfson-Royal Society award to Professor P. F. McMillan at the Royal Institution of Great Britain. This work was supported by The State Committee for Scientific Research (KBN Poland): Project No. 5 P03B 006 20.

References and Notes

(1) Wang, Y.; Patel, D. J. *Structure* **1993**, *1*, 263−282.
(2) Parkinson, G. N.; Lee, M. P. H.; Neidle, S. *Nature* **2002**, *417*, 876−880.
(3) Phan, A. T.; Patel, D. J. *J. Am. Chem. Soc.* **2003**, *125*, 15021−15027.
(4) Balagurumoorthy, P.; Brahmachari, S. K. *J. Biol. Chem.* **1994**, *269*, 21858−21869.
(5) Wang, Y.; Patel, D. J. *Biochemistry* **1992**, *31*, 8112−8119.
(6) Schmitz, K. S. *An Introduction to Dynamic Light Scattering by Macromolecules*; Academic Press: New York, 1990.
(7) Berne, B. J.; Pecora, R. *Dynamic Light Scattering with Applications to Chemistry, Biology and Physics*; Dover Publications Inc.: New York, 2000.
(8) Lin, S. C.; Lee, W. I.; Schurr, J. M. *Biopolymers* **1978**, *17*, 1041−1064.
(9) Tivant, T.; Turq, M.; Drifford, F.; Magdelenat, R.; Menez, R. *Biopolymers* **1983**, *22*, 643−662.
(10) Schmitz, K. S. *Macromolecules* **1994**, *27*, 3442−3443.
(11) Banachowicz, E.; Gapiński, J.; Patkowski, A. *Biophys. J.* **2000**, *78*, 70−78.
(12) Rotne, J.; Prager, S. *J. Chem. Phys.* **1969**, *50*, 4831−4837.
(13) Kankia, B. I.; Marky, L. A. *J. Am. Chem. Soc.* **2001**, *123*, 10799−10804.
(14) Guschlbauer, W.; Chantot, J. F.; Thiele, D. *J. Biomol. Struct. Dyn.* **1990**, *8*, 491−511.
(15) Chen, F.-M. *Biochemistry* **1992**, *31*, 3769−76.
(16) Kankia, B. I.; Marky, L. A. *J. Am. Chem. Soc.* **2001**, *123*, 10799−10804.
(17) Deng, J.; Xiong, Y.; Sundaralingam, M. *PNAS USA* **2001**, *98*, 13665−13670.
(18) Włodarczyk, A.; Gapinski, J.; Patkowski, A.; Dobek, A. *Acta Biochim. Polonica* **1999**, *46*, 609−613.
(19) Włodarczyk, A.; Patkowski, A.; Grzybowski, P.; Dobek, A. *Acta Biochim. Polonica*. Accepted for publication.
(20) Lee, J. S. *Nucleic Acids Res.* **1990**, *18*, 6057−6060.
(21) Chowdhury, S.; Bansal, M. *J. Biomol. Struct. Dyn.* **2000**, *18*, 11−28.
(22) Manning, G. *J. Chem. Phys.* **1969**, *51*, 924−942.
(23) Ramanathan, G. V.; Woodbury, C. P. *J. Chem. Phys.* **1982**, *77*, 4133−4140.
(24) Williamson, J. R. *Annu. Rev. Biophys. Biomol. Struct.* **1994**, *23*, 703−730.
(25) Sen, D.; Gilbert, W. *Methods Enzymol.* **1992**, *211*, 191−199.
(26) Miura, T.; Thomas, G. J., Jr. *Biochemistry* **1994**, *33*, 7848−7856.
(27) Cantor, C. R.; Schimmel, P. R. *Biophysical Chemistry*; W. H. Freeman and Co.: San Francisco, CA, 1980.
(28) Marky, L. A.; Breslauer, K. J. *Biopolymers* **1987**, *26*, 1601−1620.
(29) Puglisi, J. D.; Tinoco, I., Jr. *Methods Enzymol.* **1989**, *180*, 304−324.
(30) Record, M. T.; Anderson, C. F.; Lohman, T. M. *Quarterly Rev. Biophys.* **1978**, *II 2*, 103−178.
(31) Manning, G. S. *Biopolymers* **1972**, *II*, 937−949.
(32) Jing, N.; Rando, R. F.; Pommier, Y.; Hogan, M. E. *Biochemistry* **1997**, *36*, 12498−12505.
(33) Hardin, C. C.; Perry, A. G.; White, K. *Biopolymers* **2001**, *56*, 147−194.